Mapping hydrothermally altered rocks on Mount Rainier, Washington, with Airborne Visible/Infrared Imaging Spectrometer (AVIRIS) data

James K. Crowley*
U.S. Geological Survey, M.S. 954, Reston, Virginia 20192
David R. Zimbelman*
Mount Rainier National Park, Ashford, Washington 98304

ABSTRACT

Mount Rainier has produced numerous Holocene debris flows, the largest of which contain clays and other minerals derived from hydrothermally altered rocks on the volcano's edifice. Imagery from an advanced airborne sensor was used to map altered rocks at Mount Rainier and demonstrates their distinctly nonuniform distribution. The mapping of altered rocks helps to identify edifice failure surfaces and to recognize the source areas for the largest debris flow events. Remote sensing methods like those used at Mount Rainier can enhance ground-based mapping efforts and should prove useful for rapidly identifying hazardous sectors at other volcanoes.

INTRODUCTION

Hydrothermally altered rocks on stratovolcanoes are closely linked to edifice failures and the generation of destructive volcanic debris flows (Scott et al., 1995; Lopez and Williams, 1993). Altered rocks (1) form zones of weakness along fractures, dikes, and bedding surfaces, and (2) contain hydrous clay minerals that contribute to the formation of large "cohesive" debris flows that can travel many tens of kilometres (Scott et al., 1995). As illustrated by the 1980 edifice failure and eruption at Mount St. Helens (Lipman and Mullineaux, 1981) and the disastrous 1985 debris flows derived from Nevado del Ruiz volcano, Colombia (Lopez and Williams, 1993), volcanic mass-wastage events of catastrophic proportions are not uncommon. Edifice failures and destructive debris flows can be triggered by eruptions or earthquakes, but can also occur without any precursory activity (Scott et al., 1995; Lopez and Williams, 1993).

Mount Rainier has generated many large prehistoric debris flows, and future flows present significant risks to local communities. Holocene debris-flow deposits from Mount Rainier include the ca. 5.6 ka. Osceola Mudflow, which traveled as far as Puget Sound, near Tacoma, Washington, ~113 km downstream from the Mount Rainier summit (Crandell, 1971; Scott et al., 1995). Because of the potential hazards, and a paucity of available geologic data, Mount Rainier was designated as a Decade Volcano study area (National Research Council, 1994). Determining the distribution, intensity, and style of the alteration was identified as a priority concern by the National Research Council, and mapping hydrothermally altered edifice materials has recently been undertaken (Frank, 1995; Zimbelman et al.,1994, 1995; Zimbelman, 1996). This paper describes remote sensing methods that helped to support ground-based mapping activities at Mount Rainier and highlights how such methods might be used to identify hazardous sectors on other stratovolcanoes.

The National Aeronautics and Space Administration (NASA) Airborne Visible/Infrared Imaging Spectrometer (AVIRIS) used in this study collects detailed radiance spectra for every spatial pixel in a remotely sensed image (Vane and Goetz, 1993). AVIRIS is flown on the high-altitude NASA ER-2 aircraft and records radiance data in 224 closely spaced spectral bands spanning the visible to short-wave infrared (0.4–2.5 μm) wavelength range. AVIRIS images cover a swath ~11 km wide, and each image pixel represents an ~20 × 20 m area on the ground. The AVIRIS combination of high spatial and spectral resolution enables remote-sensing identification of many minerals with diagnostic spectral features. For example, clays and hydrous sulfate minerals, including those of hydrothermal origin, typically display spectral features near 1.4, 1.9, and 2.1–2.4 μm related to vibrations of structural hydroxyl groups and molecular water (Hunt and Salisbury, 1970). Iron-bearing minerals commonly exhibit broad spectral features in the 0.4–1.2 μm wavelength region due to electronic transitions in Fe^{3+} and Fe^{2+}, and to Fe-O charge transfer in Fe-oxides and oxyhydroxides. Further discussion of the origins of visible to short-wave infrared spectral features can be found in Hunt and Salisbury (1970). A review of several other geologic studies involving AVIRIS data is given by Vane and Goetz (1993).

STUDY AREA

Mount Rainier is located in south-central Washington about 60 km southeast of the city of Tacoma. Like other active Cascade Range volcanoes, Mount Rainier is a geologically young feature (oldest flows formed ca. 0.5 Ma.), constructed of hundreds of andesitic to dacitic lava flows, interbedded breccias, and ash deposits (Fiske et al., 1963; Sisson, 1995). The volcano is built upon a deeply eroded Tertiary volcano-plutonic terrain, consisting mainly of basaltic andesite, rhyodacitic ash-flow tuff, granodiorite, and granite.

Three general types of altered rock were previously identified at Mount Rainier (Zimbelman, 1996). The most important type from the standpoint of volcanic hazards consists of kaolin and smectite clay, sulfate, and silica minerals, and occurs as replacements and fracture fillings in the volcanic rocks of the edifice (Zimbelman et al., 1994, 1995; Zimbelman, 1996). A second type of altered rock is characterized by iron-oxide enrichment of porous flow tops and breccias, evidently related to the degassing of flows shortly after their extrusion. This "vapor phase" alteration is not controlled by structural features, is widely distributed across the mountain, and does not appear to represent focused or prolonged circulation of hydrothermal fluids. The third major type of altered rock at Mount Rainier consists of chlorite, sericite, quartz, and/or tourmaline within porphyry-style breccias, veins, and stockworks in Tertiary extrusive and intrusive rocks that underlie the edifice (Zimbelman, 1996).

DATA AND METHODS

AVIRIS images of Mount Rainier were acquired on July 19, 1994, at approximately 11:00 A.M. Pacific Daylight Time (Fig. 1). The radiance data provided by the NASA Jet Propulsion Laboratory were first corrected for atmospheric absorption and solar irradiance effects by using a technique developed by Gao and Goetz (1990). The data were then calibrated to surface reflectance by using a laboratory measured reflectance spectrum of an unaltered volcanic rock collected on the lower flanks of Mount Rainier. The laboratory spectrum was divided by the AVIRIS image spectrum for the same area, generating a set of calibration factors, which were then multiplied through the entire data set.

Two different analysis procedures were applied to the AVIRIS reflectance data set. The first procedure, spectral band fitting, compares a series of

*E-mail: Crowley, jcrowley@aster2.er.usgs.gov; Zimbelman, hazard@gorge.net.

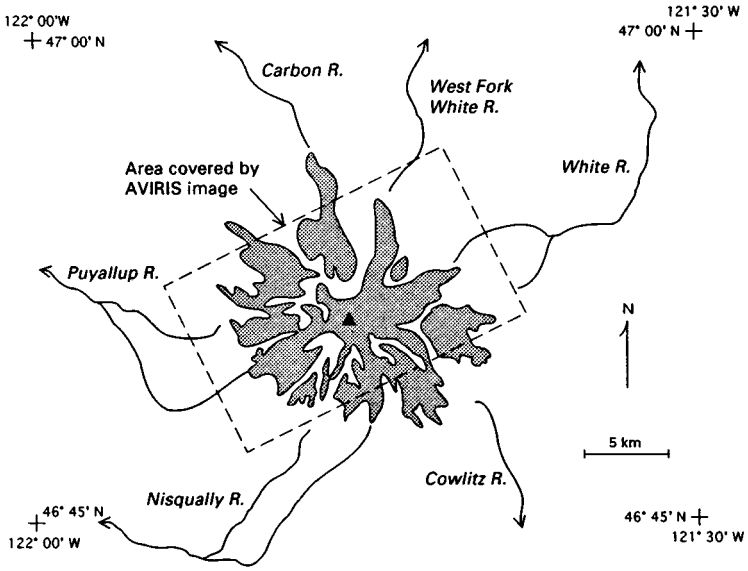

Figure 1. Location map showing Mount Rainier and surrounding major river drainages. Dashed outline indicates Airborne Visible/Infrared Imaging Spectrometer coverage. Approximate extent of glacial ice indicated by shading. The summit is marked by a black triangle.

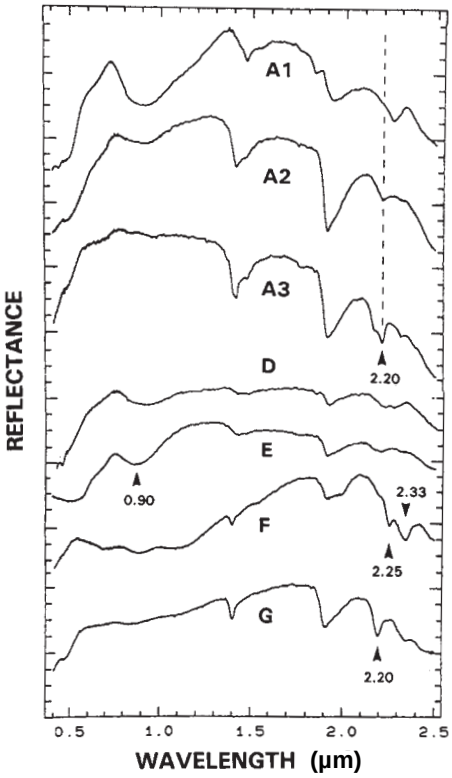

Figure 2. Laboratory diffuse reflectance spectra of Mount Rainier field samples. A1, natrojarosite-rich sample from Sunset Amphitheater; A2, natroalunite- and smectite-rich sample from upper Puyallup Cleaver; A3, kaolinite- and natroalunite-bearing sample from Sunset Amphitheater; D, cristobalite-rich sample from upper Jeanette Heights; E, goethite-bearing sample from Puyallup Cleaver; F, chlorite-rich sample from west of Tokaloo rock; G, sericite-rich sample from Copper Mountain. Table 1 gives a more detailed mineralogical description of these samples. Spectra are offset vertically for viewing purposes. Tick marks on vertical axis indicate reflectance intervals of 5%.

previously measured mineral or rock reference spectra to each AVIRIS pixel spectrum and identifies a single spectrally dominant material that best fits each pixel (Clark et al., 1990). The second procedure, linear spectral unmixing, evaluates each AVIRIS spectrum in terms of linear combinations of "pure" spectral end members—generally minerals (Boardman, 1993). The combination of end members giving the best match for each pixel is calculated and displayed. To produce the initial image results, the spectral band fitting procedure was used in conjunction with a pre-existing library of alteration mineral spectra. From these images spectra representing each of the main alteration types, as well as spectra of snow and vegetation, were extracted and used in the spectral unmixing method. This approach identified materials that were not contained in the original spectral library and also better defined altered rocks present in subpixel mixtures with vegetation, snow, and ice.

RESULTS

Laboratory-measured spectra of representative altered rock samples from Mount Rainier (Fig. 2) closely resemble AVIRIS spectra extracted from corresponding field sites (Fig. 3). The spectra are keyed to lettered field locations indicated on an AVIRIS image (Fig. 4), which shows altered rock distributions as different color patterns. Further information on sample mineralogy is provided in Table 1.

Areas of advanced argillic alteration are indicated by yellow pixels on Figure 4 and occur mainly on the upper west flank of the volcano along an arcuate escarpment known as Sunset Amphitheater, and on the nearby upper Puyallup and upper Tahoma Cleavers (Fig. 4, area A). Spectra for these areas generally show a broad feature near 2.2 μm that is caused by mixtures of amorphous silica, smectite and kaolin clays, alunite, and jarosite (Fig. 2, spectra A1, A2, A3; Fig. 3, spectrum A). Yellow pixels at the base of Tahoma Glacier (Fig. 4, area B) represent hydrothermally altered rocks from the Sunset Amphitheater that were deposited as a debris avalanche in the early twentieth century (Crandell, 1969). Yellow pixels in Glacier Basin (Fig. 4, area C1) correspond to glacial drift deposits consisting of reworked remnants of the Osceola Mudflow, whereas yellow pixels on the slopes of Steamboat Prow (Fig. 4, area C2) are a veneer of Osceola material. Although large areas of the Osceola Mudflow have been mapped in Glacier Basin (Crandell, 1969), most of the unit is obscured by vegetation cover.

The orange pixels in Figure 4 define areas of argillically altered rock, a distinct alteration subtype that was not visually differentiated from the advanced argillically altered rocks in the field. Its characteristic mineralogy is similar to that described above, except for being substantially poorer in sulfate and clay minerals (Fig. 5). Spectral curves for this alteration are subdued owing to the reduced quantity of sulfates and clays, and the somewhat more abundant silica forms, which, except for opaline quartz, are spectrally featureless (Fig. 2, spectrum D; Fig. 3, spectrum D). The sulfate- and clay-poor argillic alteration is generally exposed on the lower western and northeastern flanks of the volcano in flows that are older than those nearer to the summit (Sisson, 1995). Prominent areas of this alteration include upper Jeanette Heights (Fig. 4, area D1) and St. Elmo Pass (Fig. 4, area D2), both of which have east-northeast fracture systems and associated large through-going dikes that served to channel the hydrothermal circulation and attendant alteration processes (Zimbelman, 1996). Several small deposits of glacial drift composed of reworked altered material are also evident in Figure 4 northwest of Jeanette Heights.

Red pixels in Figure 4 depict areas of vapor phase alteration with characteristic Fe-oxide (goethite) absorption bands near 0.90 μm (Fig. 2, spectrum E; Fig. 3, spectrum E). Green pixels in Figure 4 represent areas of chloritic alteration in Tertiary rocks at the base of the edifice. Chloritized rocks show strong 2.25 and 2.33 μm absorption features characteristic of Mg-rich chlorite (Fig. 2, spectrum F; Fig. 3, spectrum F). This type of alteration is particularly evident to the west of Tokaloo Rock (Fig. 4, area F1), and at Glacier Island and Pyramid Peak (Fig. 4, area F2). Chlorite is sometimes present in mixtures with sericite, represented as magenta pixels (Fig. 4, area G), and displaying an additional narrow spectral feature at 2.2 μm (Fig. 2, spectrum G; Fig. 3, spectrum G). Many of the chlorite- and sericite-rich rocks have at least partial vegetation cover, and

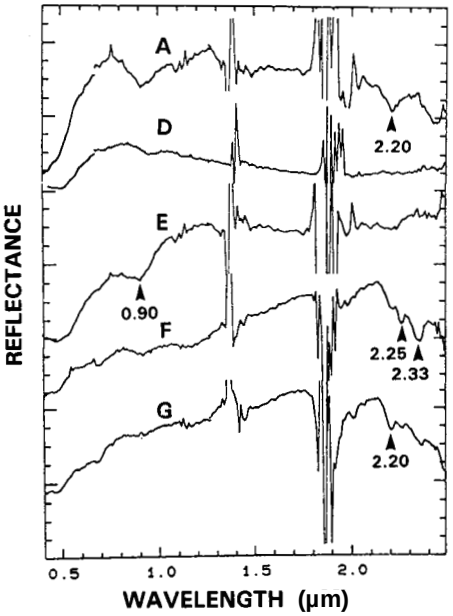

Figure 3. Airborne Visible/Infrared Imaging Spectrometer spectra extracted at selected field sample locations and used in spectral unmixing analysis. Each spectral curve represents an average of three to eight individual pixel spectra. A, clay- and sulfate-rich advanced argillic alteration in Sunset Amphitheater; D, clay- and sulfate-poor argillic alteration at upper Jeanette Heights; E, iron-oxide-bearing alteration on Puyallup Cleaver; F, chlorite-rich alteration west of Tokaloo Rock; G, sericite alteration at Copper Mountain. Spectra are offset vertically for viewing purposes. Tick marks on vertical axis indicate reflectance intervals of 5%.

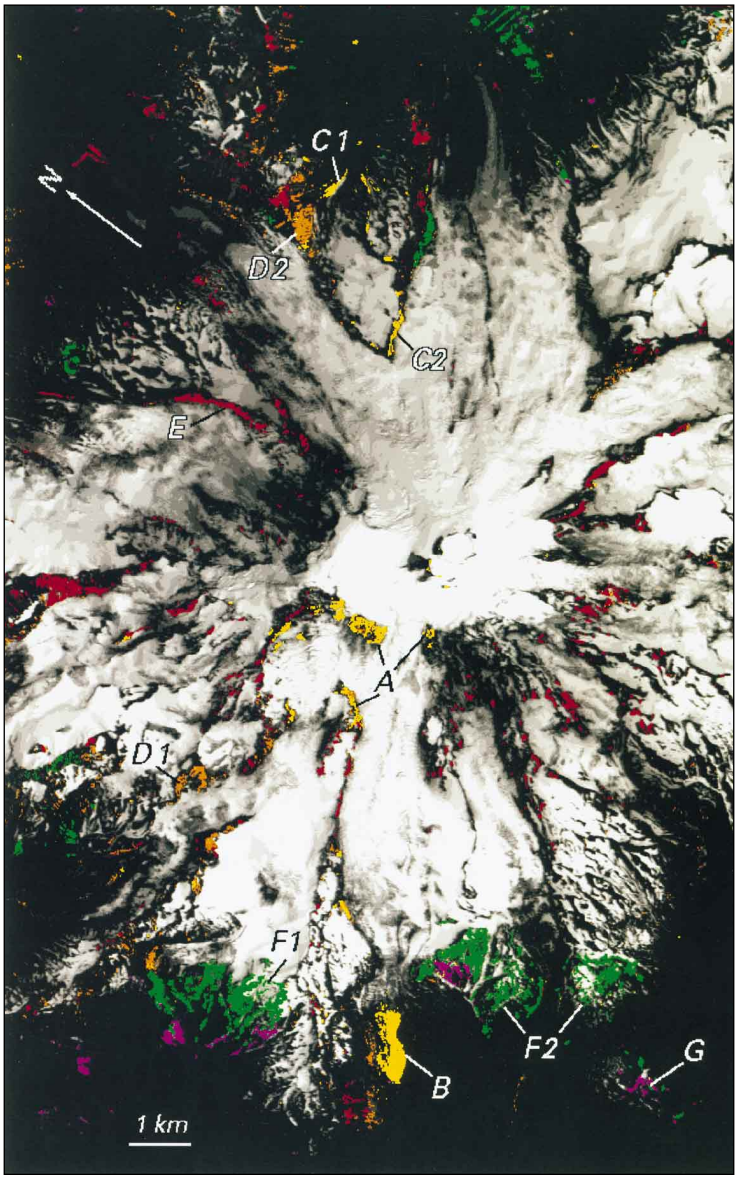

Figure 4. Airborne Visible/Infrared Imaging Spectrometer image of Mount Rainier showing different types of altered rock in different color patterns. Yellow pixels: advanced argillic alteration consisting of kaolin and smectite clays, sulfates, and various silica forms. A, pervasively altered rock in Sunset Amphitheater and at upper Puyallup and upper Tahoma Cleavers; B, early twentieth-century debris avalanche deposit derived from Sunset Amphitheater rocks; C1, glacially reworked altered material originally deposited by Osceola Mudflow; C2, veneer of Osceola Mudflow on Steamboat Prow. Orange pixels: argillically altered rock containing smaller percentage of clay and sulfate minerals than areas indicated by yellow pixels. D1, argillically altered rock at upper Jeanette Heights; D2, similar rocks exposed at St. Elmo Pass. Red pixels: iron-oxide alteration related to in situ degassing of flows. E, iron-oxide alteration at Curtis Ridge. Green pixels: chlorite alteration in Tertiary intrusive and extrusive rocks. F1, chlorite-rich area west of Tokaloo Rock; F2, chlorite-rich areas on Glacier Island (left) and Pyramid Peak (right). Magenta pixels: sericite alteration in Tertiary rocks. G, sericite-rich rocks on Copper Mountain. Scale bar is 1 km.

the spectral unmixing procedure greatly improved the ability to discern their aerial distributions.

DISCUSSION

The AVIRIS image of Mount Rainier shows that hydrothermally altered rocks occur in a broad east-west zone that bisects the volcano across its summit. This confirms the overall distribution recognized in field studies (Zimbelman et al., 1994; Zimbelman, 1996) and demonstrates the utility of remote sensing data for discerning altered rocks even in areas of steep slopes and limited exposures. In fact, the AVIRIS data depict mineralogical variations in the hydrothermally altered rocks that correspond to important variations in alteration intensity. Sulfate- and clay-rich rocks (yellow pixels on Fig. 4) represent the most intense alteration, generated where hydrothermal fluids traveled upward in the central portion of the edifice, and along subvertical, mainly east-west fractures on the volcano flanks (Zimbelman et al., 1995). The sulfate- and clay-poor rocks (orange pixels on Fig. 4) represent a lower alteration rank, probably indicating less-sustained fluid circulation and/or greater meteoric water influence in this part of the hydrothermal system. Spectral differences related to alteration mineralogy are evident in several debris avalanche and reworked drift deposits, and further investigation may permit particular debris avalanches and debris flows to be associated with particular source regions on the edifice. This could aid in understanding the development of different source regions and related changes in the hydrothermal system over time. Despite the AVIRIS sensitivity to mineralogical variations, it should be emphasized that conventional geologic mapping is still necessary to determine whether altered materials have been transported or remain in place, and to examine relationships between altered rocks and structural features (e.g., dikes and faults) that are likely to control failure modes and locations. Field studies are also needed to make volume estimates of altered rock, to collect samples for geochemical and mineralogical analyses, and to evaluate glacial undercutting and other physical factors related to debris-flow potential.

TABLE 1. MINERALOGY OF FIGURE 2 FIELD SAMPLES DETERMINED BY X-RAY DIFFRACTION

Sample	Location	Mineralogy
A1	Sunset Amphitheater	Natrojarosite, andesine
A2	Upper Puyallup Cleaver	Andesine, natroalunite, Ca-montmorillonite, kaolinite
A3	Sunset Amphitheater	Kaolinite, natroalunite, amorphous silica
D	Upper Jeanette Heights	Andesine, cristobalite, Ca-montmorillonite
E	Mid-Puyallup Cleaver	Andesine, goethite
F	West of Tokaloo Rock	Chlorite, quartz, muscovite
G	Copper Mountain	Muscovite (sericite), quartz

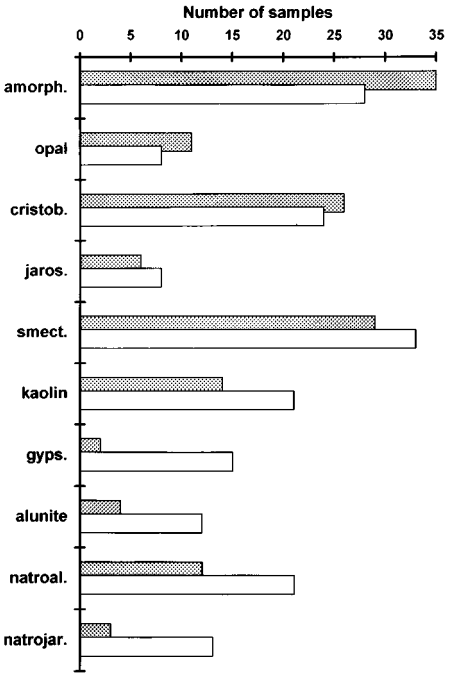

Figure 5. Comparison of X-ray diffraction analyses for hydrothermally altered Quaternary rocks (yellow and orange pixels on Fig. 4). White bars indicate minerals found in 46 samples representing areas of advanced argillic alteration (yellow pixels). Shaded bars indicate minerals found in 43 samples of argillically altered rocks (orange pixels). Note that advanced argillic samples are more likely to contain kaolin and smectite clays as well as various sulfates. Argillic samples are more likely to contain opal, cristobalite, and amorphous silica. Other minerals detected in only a few samples are omitted for clarity (see Zimbelman, 1996).

By combining results from the AVIRIS imagery and ground-based mapping studies, it is possible for the first time to directly compare the spatial distribution of altered rocks to that of postglacial debris flows. Scott et al. (1995, Tables 2 and 3) reported that large, mostly cohesive (clay-rich) debris flows have affected the Puyallup River drainage, and to a lesser extent the Nisqually River drainage, both of which are downslope from the pervasively altered Sunset Amphitheater and upper Tahoma Cleaver (Fig. 1; Fig. 4, area A). In contrast, the Carbon and Cowlitz river drainages (Fig. 1) contain fewer, mostly noncohesive, debris-flow deposits. The differences in debris-flow size, reach, behavior, and recurrence intervals are consistent with the presence or absence of hydrothermally altered rocks in the upper reaches of the respective drainage basins. On the eastern and northeastern sectors of Mount Rainier, extensive snow and ice cover, unaltered post-Osceola lava flows, and veneers of older mudflow deposits, present a complex situation that cannot be correctly inferred from the AVIRIS data alone. Ground-based mapping shows high rank alteration to be present in small exposures on the northeastern flank, and also points to three-dimensional relations between fracture zones, dikes, and altered rocks that are similar to relations seen in the better-exposed Sunset Amphitheater (Zimbelman, 1996). The sedimentary record of debris flows in the eastern and northeastern river drainages (White River, including the West Fork) indicates sustained production of both cohesive and noncohesive flows, including the voluminous Osceola Mudflow (Scott et al., 1995).

The clear link between altered rock distributions and debris-flow activity at Mount Rainier emphasizes the need for careful mapping of edifice structural and compositional features at all stratovolcanoes. Because of the difficulties inherent in mapping altered edifice materials, such studies, until recently, have not been a major component of debris-flow hazard investigations. Integrating remote sensing imagery with ground-based studies can improve their safety and efficiency, and ultimately may provide important insights for reducing risks from potentially devastating volcanic debris flows.

ACKNOWLEDGMENTS

We are grateful to K. M. Scott, T. W. Sisson, W. D. Stanley, and D. A. Swanson for their constructive reviews of this manuscript. Special thanks are also due to the National Park Service staff at Mount Rainier National Park for their continuing cooperation and assistance. Acquisition of the AVIRIS data was supported by the National Aeronautics and Space Administration Mission to Planet Earth Program.

REFERENCES CITED

Boardman, J. W., 1993, Automating spectral unmixing of AVIRIS data using convex geometry concepts, *in* Summaries of the Fourth Annual JPL Airborne Geosciences Workshop, Oct. 25–29, 1993: Jet Propulsion Laboratory Special Publication 93-26, p. 11–14.

Clark, R. N., Gallagher, A. J., and Swayze, G. A., 1990, Material absorption band depth mapping of imaging spectrometer data using a complete shape least-squares fit with library reference spectra, *in* Proceedings of the Second AVIRIS workshop: Jet Propulsion Laboratory Publication 90-54, p. 176–186.

Crandell, D. R., 1969, Surficial geology of Mount Rainier National Park, Washington: U.S. Geological Survey Bulletin 1288, 41 p.

Crandell, D. R., 1971, Postglacial lahars from Mount Rainier volcano, Washington: U.S. Geological Survey Professional Paper 677, 75 p.

Fiske, R. S., Hopson, C. A., and Waters, A. C., 1963, Geology of Mount Rainier National Park, Washington: U.S. Geological Survey Professional Paper 444, 93 p.

Frank, D., 1995, Surficial extent and conceptual model of hydrothermal system at Mount Rainier, Washington: Journal of Volcanology and Geothermal Research, v. 65, p. 51–80.

Gao, Bo-Cai, and Goetz, A. F. H., 1990, Column atmospheric water vapor and vegetation liquid water retrievals from airborne imaging spectrometer data: Journal of Geophysical Research, v. 95, p. 3549–3564.

Hunt, G. R., and Salisbury, J. W., 1970, Visible and near-infrared spectra of minerals and rocks: I. Silicate minerals: Modern Geology, v. 1, p. 283–300.

Lipman, P. W., and Mullineaux, D. R., eds., 1981, The 1980 eruptions of Mount Saint Helens, Washington: U.S. Geological Survey Professional Paper 1250, 844 p.

Lopez, D. L., and Williams, S. N., 1993, Catastrophic volcanic collapse: Relation to hydrothermal processes: Science, v. 260, p. 1794–1796.

National Research Council, 1994, Mount Rainier: Active Cascade volcano: Washington, D.C., National Academy Press, 114 p.

Scott, K. M., Pringle, P. T., and Vallance, J. W., 1995, Sedimentology, behavior, and hazards of debris flows at Mount Rainier, Washington: U.S. Geological Survey Professional Paper 1547, 56 p.

Sisson, T. W., 1995, An overview of Mount Rainier's volcanic edifice [abs.]: Eos (Transactions, American Geophysical Union), Abstracts Volume, p. 93.

Vane, G., and Goetz, A. F. H., 1993, Terrestrial imaging spectrometry: Current status, future trends: Remote Sensing of Environment, v. 44, p. 117–126.

Zimbelman, D. R., 1996, Hydrothermal alteration and its influence on volcanic hazards—Mount Rainier, Washington, a case history [Ph.D. thesis]: Boulder, University of Colorado, 384 p.

Zimbelman, D. R., Sisson, T. W., Whitney, C. G., and Esposito, K. J., 1994, Relationship of hydrothermal alteration to volcanic hazards at Mount Rainier, Washington—Preliminary results: Geological Society of America Abstracts with Programs, v. 26, no. 7, p. A–114.

Zimbelman, D. R., Rye, R. O., and Plumlee, G. S., 1995, Single-stage hydrothermal alteration at Mount Rainier volcano, Washington: International Union of Geodesy and Geophysics, 21st General Assembly, Abstracts, p. A467–A468.

Manuscript received September 23, 1996
Revised manuscript received February 14, 1997
Manuscript accepted March 6, 1997